Report of Investigation 2019 *Draft*

LANDSLIDE HAZARD EVALUATIONS FOR MULTI-HAZARD RISK MAPPING IN SITKA, ALASKA

Trent D. Hubbard, Ronald P. Daanen, and De Anne S.P. Stevens

Published by
STATE OF ALASKA
DEPARTMENT OF NATURAL RESOURCES
DIVISION OF GEOLOGICAL & GEOPHYSICAL SURVEYS
2019

Cover. Damage from 2015 landslides in Sitka, Alaska.

LANDSLIDE HAZARD EVALUATIONS FOR MULTI-HAZARD RISK MAPPING IN SITKA, ALASKA

Trent D. Hubbard, Ronald P. Daanen, and De Anne S.P. Stevens

Report of Investigation 2019 *Draft*

State of Alaska
Department of Natural Resources
Division of Geological & Geophysical Surveys

STATE OF ALASKA
Michael J. Dunleavy, Governor

DEPARTMENT OF NATURAL RESOURCES
Corri A. Feige, Commissioner

DIVISION OF GEOLOGICAL & GEOPHYSICAL SURVEYS
Steve Masterman, State Geologist and Director

Publications produced by the Division of Geological & Geophysical Surveys (DGGS) are available for free download from the DGGS website (dggs.alaska.gov). Publications on hard-copy or digital media can be examined or purchased in the Fairbanks office:

Alaska Division of Geological & Geophysical Surveys
3354 College Rd., Fairbanks, Alaska 99709-3707
Phone: (907) 451-5010 Fax (907) 451-5050
dggspubs@alaska.gov | dggs.alaska.gov

DGGS publications are also available at:
Alaska State Library,
Historical Collections & Talking Book Center
395 Whittier Street
Juneau, Alaska 99811

Alaska Resource Library and Information Services (ARLIS)
3150 C Street, Suite 100
Anchorage, Alaska 99503

Suggested citation:
Hubbard, T.D., Daanen, R.P., and Stevens, D.S.P., 2019, Landslide hazard evaluation for multi-hazard risk mapping in Sitka, Alaska: Alaska Division of Geological & Geophysical Surveys Report of Investigation.

Contents

Figures

Tables

LANDSLIDE HAZARD EVALUATIONS FOR MULTI-HAZARD RISK MAPPING IN SITKA, ALASKA

Trent D. Hubbard,[1] Ronald P. Daanen,[1] and De Anne S.P. Stevens[1]

Abstract

The threat of landslides poses a great safety and financial risk to people and infrastructure in many communities throughout Alaska, including the City and Borough of Sitka. To better inform Sitka of potential landslide hazards and increase the City's hazard resiliency, the Alaska Division of Geological & Geophysical Surveys created maps of historical landslides, shallow landslide susceptibility, and simulated debris flow runout to assess landslide hazards in and around the community. The historical landslide inventory map integrates existing mapped landslides with additional landslides identified using newly acquired high-resolution lidar. A shallow-landslide susceptibility map was created following protocols similar to those developed by the Oregon Department of Geology and Mineral Industries, incorporating, landslide inventory data, geotechnical data, and lidar slope data to calculate Factor of Safety (FOS), which was used to categorize landslide susceptibility. The debris flow runout map was generated using the computer model LaharZ, which simulates runout extent based on physical parameters derived from three documented debris flows in the Sitka area. We used catchment size and slope derived from lidar to scale each catchment to the volume of debris. Data from the three analyses were combined to produce an integrated landslide hazards map intended to depict overall risk. The results provide important information about landslide hazards that can help guide planning and future investigations. The maps are not intended to predict landslides, and site-specific detailed investigations should be conducted prior to development in vulnerable areas.

INTRODUCTION

On August 18, 2015, heavy rainfall and wind resulted in numerous landslides in and around Sitka, Alaska. More than 45 landslides were initiated during this event and documented on Chichagof and Baranof Islands. Four debris flows impacted roads and infrastructure in Sitka, and the southernmost of two flows at Kramer Avenue took the lives of three residents. This tragedy highlighted the importance of understanding landslide risk to inform mitigation efforts, guide future development activities, and protect public safety in and around Sitka.

To assist the City and Borough of Sitka in becoming more resilient to landslide hazards and to inform the Sitka Multi-Hazard Risk MAP, the Alaska Division of Geological & Geophysical Surveys (DGGS) was funded in 2016 by the Federal Emergency Management Agency (FEMA) Cooperating Technical Partners (CTP) Program to create a historical debris flow inventory map, debris flow susceptibility maps, and simulated debris flow runouts to assess landslide susceptibility for an area of interest (AOI) including the City of Sitka (figure 1). The AOI was chosen in consultation with the City of Sitka and includes priority areas within

[1]Alaska Division of Geological & Geophysical Surveys, 3354 College Road, Fairbanks, Alaska 99709-3707.

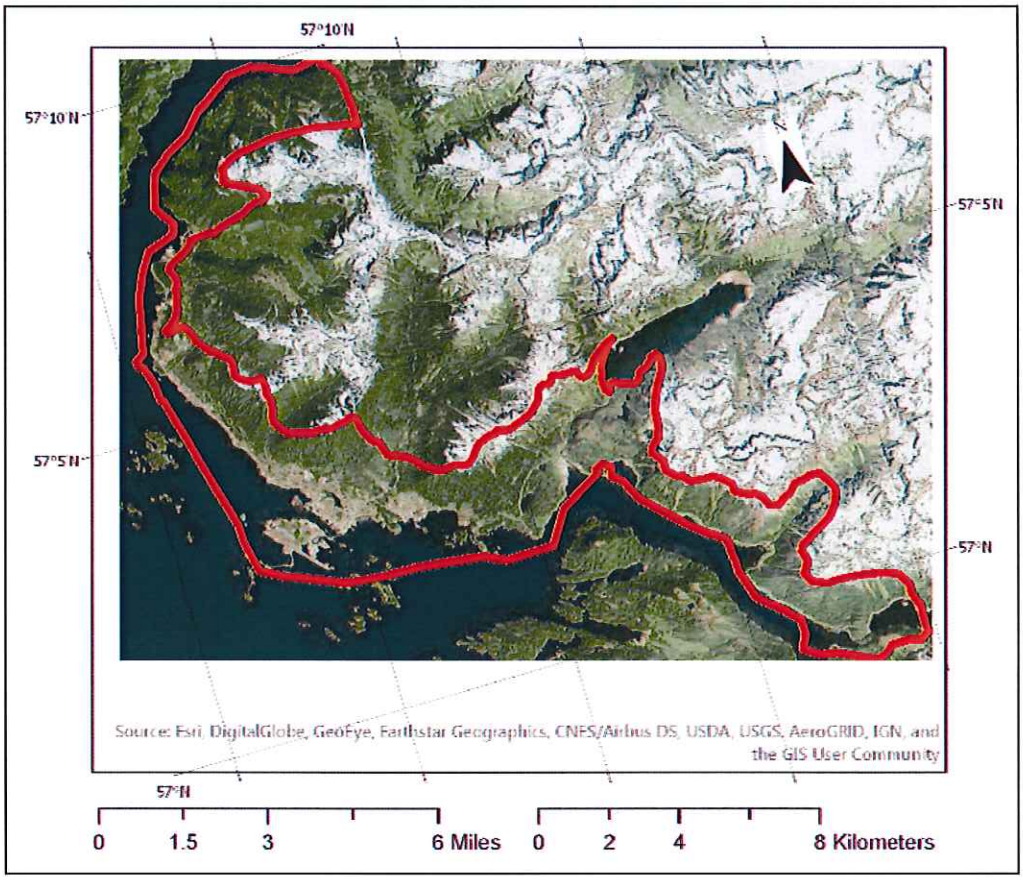

Figure 1. Map showing Sitka landslide evaluation project area of interest (red outline), which includes the current community footprint, critical hydroelectric infrastructure, and near-term future development areas.

areas of lidar data collected in 2016 and 2018. This report describes the datasets and methods used in this study. We discuss the mapping and modeling results and make recommendations for increasing Sitka's landslide hazard resiliency.

METHODS

Landslide Inventory

To develop a comprehensive landslide inventory, DGGS (1) collected and organized existing information about previously identified landslides, (2) obtained remotely sensed data to evaluate the accuracy, extent, and location of identified landslides, (3) acquired and processed high-resolution lidar (Light Detection and Ranging) elevation data, (4) identified additional historical landslide areas using lidar data, (5) compiled all landslide information, with appropriate attribute information, into a geodatabase, and (6) generated a landslide inventory map.

Collect Existing Landslide Information

DGGS collected existing data about landslide location and extent and assembled a geodatabase. Available data included geospatial landslide inventory data for the Sitka area—part of a larger dataset for the Tongass National Forest (U.S. Department of Agriculture [USDA], 2017)—and previous work by DGGS (Gould and others, 2015). The DGGS work was carried out in cooperation with the Sitka Geoscience Task Force, an informal scientific "think tank" assembled in response to the deadly

August 2015 landslides. We identified landslides in both datasets by interpreting remotely sensed data, including satellite imagery and historical air photos, and field investigations.

Imagery Acquisition and Evaluation of Existing Landslide Inventory

Available remotely sensed data, including satellite imagery, historical air photos, Interferometeric Synthetic Aperture Radar (IFSAR), and multiple epochs of lidar were identified and obtained. We used this data to evaluate previously inventoried landslides for accuracy and to identify any additional features. We modified outlines of landslides from the inventory and added new landslides as necessary.

Lidar Acquisition and Processing

In early 2016, DGGS contracted a lidar survey from the U.S. Army Corps of Engineers Cold Regions Research and Engineering Lab (CRREL). The lidar data was meant to be used to create bare-earth digital elevation models (DEMs) of the ground surface to identify landslides that could not be recognized in other imagery because of dense vegetation cover. Unfortunately, the ground point density of the 2016 CRREL lidar mission was not adequate for constructing detailed ground models needed for landslide identification in much of this steep, densely forested terrain. In order to produce bare earth DEMs with sufficient ground point density for mapping landslides, DGGS conducted a new lidar survey in May 2018. We processed the data in-house and produced ground modeled surfaces. On steep densely vegetated slopes we were able to obtain ~3.5 ground-classified points per $1m^2$ with approximately 100 non-ground classified points for every ground-classified point. Our resulting modeled ground surfaces proved excellent for identifying landslide deposits in this complex terrain.

Lidar Interpretation

We used hillshade and slopeshade images along with 10 meter-interval contours derived from lidar DEMs, in combination with other available imagery, to identify landslide deposits based on their geomorphic characteristics. Descriptions of characteristic landslide features and other useful information for identification can be found in Varnes (1978).

Creating the Inventory

Using methodology similar to that of the Oregon Department of Geology and Mineral Industries (Burns and Madin, 2009), DGGS combined lidar DEMs with derivative hillshade and slopeshade images and other remotely sensed data to refine the existing landslide inventory for accuracy and completeness, and to identify additional landslides. All data were incorporated into a geospatial database with associated attribute data. Except for a few complex rock falls, landslides in this region are almost exclusively debris flows. Many of the debris flows have associated debris flow fans. We recognized debris flows generated by two initiation processes: (1) shallow landslides that mobilize as debris flows as they become channelized, and (2) debris flows generated by runoff, where overland flow mobilizes colluvial slope deposits and material stored in avalanche chutes and steep channels.

Landslides were classified as historical and/or active if the date of movement occurred within the last 50 years, as determined from imagery interpretation or by documentation. Landslides were identified as prehistoric or ancient if movement occurred more than 50 years ago as determined from imagery interpretation. The resultant landslide inventory map is shown on sheet 1.

LANDSLIDE SUSCEPTIBILITY

DGGS developed a landslide susceptibility map for the Sitka area using methods modified from Burns and others (2012), who describe the protocol for shallow-landslide susceptibility mapping used by the State of Oregon. This methodology requires (1) creating a Factor of Safety (FOS) map using geospatial and geotechnical data, and (2) generating a landslide susceptibility map

by combining the FOS map with data from the landslide inventory map.

Factor of Safety Map

Factor of Safety is the relationship between forces acting to move material downslope and forces acting to resist movement, and is used to approximate landslide susceptibility. In general, the greater the forces acting to move the material downslope relative to those resisting movement, the lower the FOS and the greater likelihood landslides may occur.

FOS can be approximated using geotechnical information about earth material and the slope of the land surface.

The equation is:

$$FOS = \frac{c'}{\gamma t \sin \alpha} + \frac{\tan \Phi}{\tan \alpha} - \frac{m\gamma_w \tan \Phi}{\gamma \tan \alpha}$$

Where:

c' = cohesion (effective)

Φ = angle of internal friction (effective)

γ = soil density (unit weight)

γ_w = groundwater density (unit weight)

t = depth to failure surface

m = groundwater depth ratio

α = slope angle

To determine FOS, we used soils data obtained from the U.S. Department of Agriculture (USDA; 2018) and other sources to calculate or approximate each of the variables in the above equation. Although the USDA data was the most complete dataset and was chosen for this analysis, data values were validated using other references (Yehle, 1974; Filz, 1982; Schroeder, 1983; Harp and others, 2006; Golder Associates, 2008; Shannon & Wilson, Inc., 2016).

DGGS classified geospatial soil data according to parent material ("geologic unit"), and then used the associated geotechnical information for each soil unit to calculate a representative saturated soil density for each geologic unit. To be conservative and anticipate worst-case scenarios, we used the highest value of dry bulk density to calculate saturated bulk density.

The landslides in this area are shallow, so the depth to failure was estimated as depth to bedrock using USDA data. To anticipate worst-case scenarios and because debris flows often occur during heavy rain events, we assumed the groundwater depth ratio to be one (implying fully saturated conditions). Values used to calculate FOS for each geologic unit are shown in table 1.

Representative angle of internal friction, cohesion, and groundwater density were assigned to each geologic unit based on sample analyses from field data collected by other workers in the region (Filz, 1982; Schroeder, 1983). Values were then verified using typical values from other published data (Harp and others, 2006; Burns and others, 2012; Geotechdata.info, 2013; Shannon & Wilson, Inc., 2016). Published cohesion values are highly variable in the literature so we chose representative values closer to those of Filz (1982) and Schroeder (1983), who analyzed representative samples from southeast Alaska.

Geotechnical properties were assumed constant for each geologic unit, but slope varies so FOS was calculated independently for ranges of slope within each geologic unit. Table 2 shows an example of FOS calculated for volcanic ash at 0.5-degree slope intervals between 13 and 28.5 degrees.

To display the FOS results in map space, geologic parent material vector polygons derived from the USDA data were converted to raster format. Raster cell values were assigned based on the attribute value of the geologic parent material polygon at the center of each cell. A series of operations were then performed to create a new raster in which each 1 m (~3.3 ft) cell was assigned an FOS value dependent on the type of geologic material and the slope within that raster cell (obtained from

Table 1. Geotechnical properties used to calculate FOS for each geologic unit.

Map ID	Geologic Unit	Effective cohesion		Effective Angle of Internal Friction	Unit weight of soil		Unit weight of water		Depth to Failure		Groundwater Depth Ratio
		lb/ft²	kPa	Degrees	lb/ft³	kN/m³	lb/ft³	kN/m³	ft	m	
1	Alluvium	140.0	6.7	36	101.1	15.9	64.0	10.1	6.6	2.0	1
2	Bedrock	280.0	13.4	35	103.6	16.3	64.0	10.1	1.0	0.3	1
3	Colluvium	50.0	2.4	22	102.3	16.1	64.0	10.1	1.4	0.4	1
4	Colluvium and/or glaciofluvial deposits	90.0	4.3	29	106.7	16.8	64.0	10.1	2.7	0.8	1
5	Colluvium and/or residuum	50.0	2.4	22	103.6	16.3	64.0	10.1	2.6	0.8	1
6	Colluvium derived from sandstone and/or residuum weathered from sandstone	50.0	2.4	22	108.6	17.1	64.0	10.1	1.7	0.5	1
7	Glaciofluvial deposits	140.0	6.7	36	113.6	17.8	64.0	10.1	5.3	1.6	1
8	Gravelly alluvium	50.0	2.4	36	101.1	15.9	64.0	10.1	0.8	0.2	1
9	Organic material	80.0	3.8	23	123.6	19.4	64.0	10.1	5.9	1.8	1
10	Organic material over residuum	80.0	3.8	23	82.4	12.9	64.0	10.1	1.4	0.4	1
11	Volcanic ash	140.0	6.7	20	126.0	19.8	64.0	10.1	2.7	0.8	1

lidar elevation data). For example, a raster cell of volcanic ash with slope of 19 degrees has an FOS of 1.50 (table 2).

Based on the work of Burns and others (2012), areas with FOS values > 1.5 are classified as low landslide susceptibility, FOS values from 1.25 to 1.5 are classified as moderate landslide susceptibility, and FOS values < 1.25 are classified as high landslide susceptibility. Table 2 shows an example of landslide susceptibility based on slope for the volcanic ash geologic unit. Shannon & Wilson (2016) estimate that debris flows in and near Sitka are initiated on slopes of about 70 percent (~36 degrees), while our susceptibility analysis suggests volcanic ash on lesser slopes may be susceptible to failure. It is important to remember that our parameters are deliberately conservative, and site-specific investigations by qualified engineers are needed due to the generalized nature of our analysis.

Because the slope map used to calculate FOS was created from high-resolution lidar data with 1 m (~3.3 ft) cell size, small-scale, low-relief

Table 2. Example of calculated FOS values for volcanic ash parent material.

Slope	FOS
13.0	2.20
13.5	2.11
14.0	2.04
14.5	1.97
15.0	1.90
15.5	1.84
16.0	1.78
16.5	1.73
17.0	1.68
17.5	1.63
18.0	1.59
18.5	1.54
19.0	1.50
19.5	1.46
20.0	1.43
20.5	1.39

Slope	FOS
21.0	1.36
21.5	1.33
22.0	1.30
22.5	1.27
23.0	1.24
23.5	1.22
24.0	1.19
24.5	1.17
25.0	1.14
25.5	1.12
26.0	1.10
26.5	1.08
27.0	1.06
27.5	1.04
28.0	1.02
28.5	1.00

	Low landslide susceptibility
	Moderate landslide susceptibility
	High landslide susceptibility

features (e.g., ditches) that do not pose a significant landslide hazard can be misclassified as having moderate or high landslide susceptibility. In order to account for this, we used an ArcGIS Pro focal relief tool to reduce anomalous areas identified as high or moderate susceptibility associated with such features, thus reducing landslide susceptibility overestimation. After several iterations, we found that surface smoothing using the focal statistics tool with a range of 3 x 5 m (~9.8 x ~16.4 ft) and a relief of less than 2 m (6.6 ft) produced best results for removing such features. These values are consistent with the work of Burns and others (2012).

We found that, even after running the focal statistics tool, features such as buildings may still be classified as high or moderate susceptibility because lidar-based elevation models do not distinguish between elevation changes of man-made and natural features that have steep sides or slopes. Extensive GIS manipulation and additional field work would be required to locate all the existing structures and remove them from the DEM, and further smoothing would also remove areas properly classified as high or moderate susceptibility. Thus we have retained these features in the susceptibility map as the most conservative approach.

Landslide Susceptibility Map

To create the landslide susceptibility map, we first converted the landslide inventory map from vector to raster format in which each cell in the raster that was part of a landslide polygon was classified as high susceptibility and each cell not part of a landslide polygon was classified as low susceptibility. We then combined the landslide inventory map with the post-focal statistics FOS raster map. In the combined map, all cells with landslide polygons were assigned to the high susceptibility class while all other cells retained their value in the FOS raster map. The final map is shown on sheet 2.

Our landslide susceptibility analysis is appropriate for shallow landslides that mobilize as debris flows but may not be an accurate predictor of debris flows generated by mobilization of material during runoff because of differences in how the two types of debris flows are generated. However, the landslide susceptibility maps incorporate debris flow fans, which are produced by both types of

debris flows, and thus our analysis contributes to the understanding of susceptibility from both types of slope failure.

Comprehensive landslide analysis requires evaluation of all areas upslope from hazard areas in order to account for all possible debris contributions and potential landslides. While we were able to collect lidar to the ridgeline above Sitka, weather conditions prevented us from collecting data in a few higher elevations near Starrigavin Bay and east of Harbor Mountain. These areas were generally small and our assessment still provides valuable information that helps identify potential landslide hazards in these areas.

SIMULATING DEBRIS FLOW RUNOUT

LaharZ is a computer model developed by Schilling (1998) for the U.S. Geological Survey that simulates the behavior of volcanic mudflows, known as lahars. This relatively simple computational model uses statistical descriptions of areas inundated by past mass-flow events to forecast areas likely to be inundated by hypothetical future events, and is suitable for modeling many types of debris flows. The forecasts use physically motivated and statistically calibrated power-law equations that each have a form $A = cV^{2/3}$, relating mass-flow volume (V) to planimetric or cross-sectional areas (A) inundated by an average flow as it descends a given drainage. Four parameters are necessary: (1) a starting point of debris accumulation, (2) total debris volume, and (3 and 4) two constants (C and c, cross-sectional and planimetric, respectively) describing flow characteristics. Incremental volume is calculated in sections proceeding downslope from a starting point based on debris elevation and calculated flow characteristics. LaharZ models debris flows down the steepest path of the slope (based on the DEM), filling low-lying areas until the input volume is depleted. All four debris flow parameters are important in determining the area of impact from debris runout.

The two parameters used for flow characteristics in LaharZ describe the viscosity of flowing material and how it affects the distribution of debris on the landscape. Values can range from pure water to pure rock, with water being the least viscous material and rock the most viscous. Water would generate a narrow, fast stream and travel a long distance, whereas rock debris would form a steep pile at the terminus of the debris flow. The behavior of debris flows falls between the two extremes and depends on the material grain size, distribution of debris, and the roughness of the landscape. In Sitka the debris is similar on all evaluated slopes and consists primarily of volcanic ash, glacial till, organic material, and variable amounts of woody debris (the density of large trees varies on the slopes due to the area's logging history).

In order to simulate debris flows in Sitka, we first calibrated the LaharZ parameters for flow characteristic constants C and c with the known size and volume of the August 2015 South Kramer debris flow (figure 2). We established 0.1 for the cross-sectional area (C) calculation and 55 for the planimetric area (*c*) calculation of the flow section as the best fit to the South Kramer debris flow. These differ slightly from the standard debris flow constants 0.1 and 20, respectively, and the standard lahar constants 0.05 and 200, respectively (Iverson and others, 1998). This suggests the deposits on Sitka slopes are slightly more liquid than typical debris flows, but not as liquid as a typical lahar. The calibrated parameters were also found to fit two other debris flows in the area, a small debris flow near Silver Bay, and a much larger debris flow in Starrigavan Valley.

We used debris flow volumes ranging from 900 m^3 to 48,000 m^3 (31,781 ft^3 to 1,695,104 ft^3) for our modeled catchments. These volumes represent two historical debris flows that occurred in the Sitka area: the Silver Bay debris flow of 2015 and the Starrigavan debris flow of September 2014, respectively. The volume for the Silver Bay debris flow was derived from lidar differencing between 2014

City of Sitka lidar and the 2016 CRREL lidar. The volume for the Starrigavan debris flow was derived from differencing of 2012 IFSAR and 2018 DGGS lidar. For simulations of medium-size catchments, we used the 11,000 m^3 (388,461 ft^3) volume of the South Kramer debris flow as the upper volume limit, which is derived from differencing the area of runout on the 2014 lidar and Structure from Motion (SfM) data collected by DGGS immediately after the debris flow in 2015 (DGGS Staff, 2013).

Smaller debris flows occur more often than larger ones and larger catchments produce debris flows more often than smaller ones, so we scaled the modeled debris flows by catchment size and related characteristics. Catchment scaling was accomplished using three parameters: (1) catchment area, (2) catchment mean slope, and (3) catchment maximum range in elevation. For each of the three parameters, cutoffs were chosen to divide the catchments into two groups of roughly the same number. The cutoffs chosen were 40,000 m^2 (430,556 ft^2) area, 35°mean slope, and 250 meters (~820 feet) elevation range. Scores of one or zero were then assigned to catchments with greater and lesser values, respectively, of the parameter. The three individual scores for each catchment were then added to determine catchment size categories: large, medium, and small (values ranging from three to zero). Total scores of one and zero were lumped together into the small catchment category. Volumes assigned to each class are given in table 3.

The starting points of debris flows were chosen based on geomorphological evidence of debris accumulation along a drainage. Typically this occurs at a location where the mountain slope is 20–30 degrees, but each catchment varies depending on the local debris source and vegetation. Figure 2 shows our debris flow simulations of the South Kramer slide for three different slide volumes.

In some areas where we simulated debris flows we needed to hydro-flatten or hydro-enforce our DEM model to ensure the modeled landslides moved in appropriate directions. In some cases this required filling in manmade trenches or removing

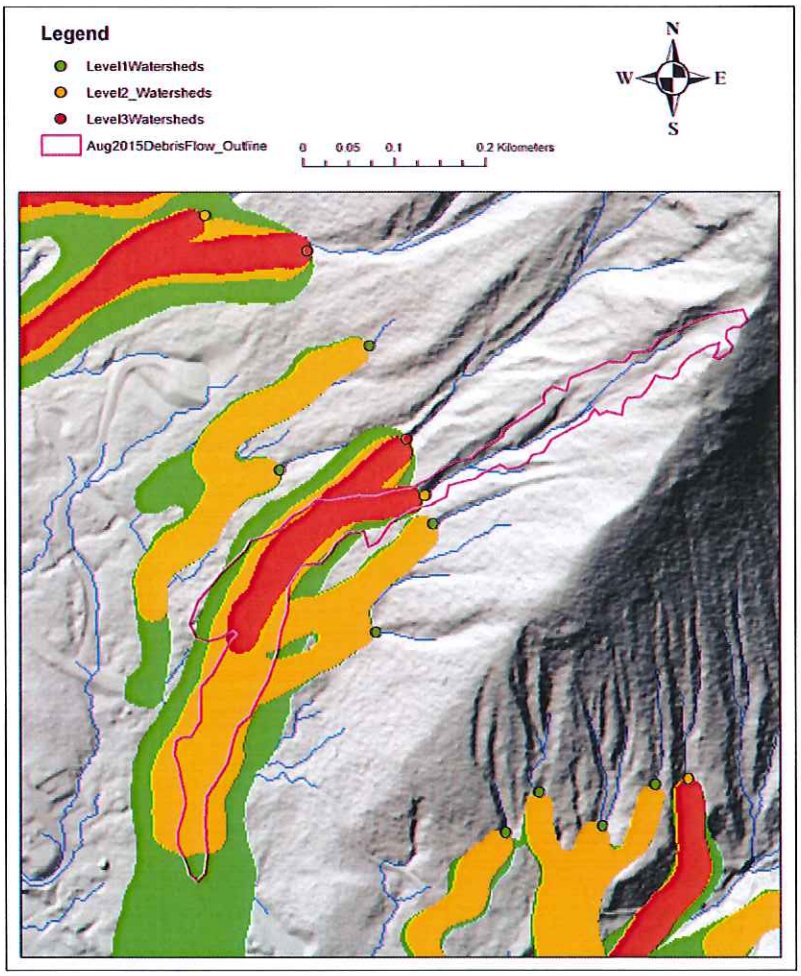

Figure 2. South Kramer debris flow simulated with LaharZ after calibration. The three colors indicate the high-medium-low volumes from table 3 for medium-size catchments and smoothened. The purple outline delineates the August 2015 South Kramer debris flow, as mapped from aerial imagery and on-the-ground GPS measurements.

small edges on road embankments that would potentially curb water movement, but not a debris flow. The sensitivity of LaharZ to small topographic features caused modeled debris flows to make unrealistic turns in response to roads and ditches before these were hydro-enforced.

The next step in the process was to smooth the simulated debris flow extents to eliminate artifacts generated by small variations in the elevation model. We used the ArcGIS focal statistics and conditional tools to create our final debris flow zones. Figure 2 shows the smoothed example at the August 2015 South Kramer slide catchment. Any area outside the colored zones will likely not experience a debris flow, but very rare cases are not included in our assessment of the debris flow hazard and an event cannot be completely ruled out for the entirety of these areas. The complete runout modeling results for the entire study area are shown on sheet 3.

LANDSLIDE SUSCEPTIBILITY ASSESSMENT

Sitka is surrounded by steep slopes and has a long history of landslides (Bishop and Stevens, 1964; Combellick and Long, 1983; Johnson and others, 2000; Becker, 2014; Harris, 2014). The current assessment is designed to help the City and Borough of Sitka identify areas of elevated debris flow risk based on historical information, available geotechnical data, elevation data from recently acquired high-resolution lidar, and debris flow runout modeling (sheet 4). There are areas where we were unable to collect detailed lidar data to the tops of ridgelines, especially in some areas east of Sitka. These areas should be further evaluated for landslide risk. Despite the data gaps, our landslide inventory, susceptibility maps, and runout models provide important data previously unavailable to Sitka.

In general, areas mapped as having elevated landslide susceptibility are primarily on and at the base of steep slopes (sheets 2 and 4). In the event of a large earthquake there is a chance of compound hazards—such as soil liquefaction on slopes—that could trigger landslides. Earthquakes can also loosen bedrock that is currently holding sediments in place.

Care should be taken before development in areas of historical landslide deposits. Many of the drainages on Sitka's steep slopes are conduits for debris, and many have debris flow fans at their base indicating one or more debris flow events occurred in the past. Most of these features were identified using remotely sensed data but have not been assessed on the ground. We recommend site-specific investigations by qualified engineers to help evaluate risk in these areas and the potential for future activity.

Table 3. Debris volume ranges per simulated flow.

Catchment Size	Volume					
	High volume-low frequency		Medium volume and frequency		Low volume- high frequency	
Large	48,000 m^3	1,695,104 ft^3	11,000 m^3	388,461 ft^3	900 m^3	31,783 ft^3
Medium	11,000 m^3	388,461 ft^3	2,500 m^3	88,287 ft^3	900 m^3	31,783 ft^3
Small	N/A	N/A	2,500 m^3	88,287 ft^3	900 m^3	31,783 ft^3

Debris flow runout modeling (sheets 3 and 4) suggests that there are many areas of concern with respect to current and planned development. We recommend that detailed engineering studies be conducted on the individual modeled debris flows to better quantify their potential size, force, and runout. To facilitate the engineering studies, we recommend developing more-detailed soils maps and collecting site-specific geotechnical data for the catchments on slopes that are at risk of generating debris flows in areas where people spend a large amount of time. These soils maps and geotechnical data can be used to more precisely calculate debris volume currently on the slopes in those catchments, and their potential for failure. The state of the forest should also be studied in these catchments in order to determine if and/or when the last debris flow occurred, and to assess the amount of woody debris in the potential debris flows these catchments could produce.

Posting signs in high-hazard areas would remind residents to be landslide-aware, particularly during significant rain events. Useful reference material and imminent debris flow warning indicators are summarized in the U.S. Geological Survey fact sheet "Debris-Flow Hazards in the United States" at https://pubs.usgs.gov/fs/fs-176-97/fs-176-97.html (web page) and https://pubs.usgs.gov/fs/fs-176-97/fs-176-97.pdf (hard copy). This general-audience brochure should be distributed to Sitka residents and visitors.

For areas under consideration for future development, the possibility of designating green space in areas of debris flow hazard and constructing engineered mitigation structures that can divert debris flows into those green spaces could be evaluated. Engineering structures require long-term maintenance and this needs to be taken into consideration.

Finally, we recommend a debris flow warning system so people can evacuate high-hazard zones during large and/or continuous rain events. Such a system is already under development in Sitka in response to the deadly August 2015 landslides. Traffic signs with flashing lights connected to the warning system could alert motorists during times when debris flow hazard is elevated. Much like tsunami warning sirens, sirens could be activated when hazardous conditions are imminent or occurring.

MAP USE AND LIMITATIONS

The landslide inventory, landslide susceptibility, debris flow runout, and integrated debris flow hazard maps were developed using the best available data, however, there are inherent limitations as discussed below. The intended use of these overview maps is to help identify the relative landslide risk in and around Sitka and to provide a basis for regional planning and increased resiliency, as well as to help identify localities where more-detailed landslide mapping is warranted. Maps are not intended for use at scales other than the published map data scale (1:20,000). Limitations of the input data and modeling methods we used to make the map are such that the map is not suitable to answer site-specific questions. The map should be used only for regional or community-scale purposes. The following is a list of specific limitations:

- Every effort has been made to ensure the accuracy of the previously-mapped landslide data, however, it is not feasible to completely verify all original input data.
- While every effort was made to map all landslides, given the limitations of available imagery, minimal field validation, and high vegetation density, it is likely that some landslides were missed or misinterpreted by map authors, even with the high-quality lidar-derived topographic data.
- The lidar-based mapping is a "snapshot" view of the current landscape, and may change as new information regarding landslides becomes available and new landslides occur.
- The FOS calculations for landslide susceptibility maps are done on one individual grid cell at a time, without regard for the adjacent grid cells.

- The focal relief method was used to try to reduce the problem of overestimation of landslide susceptible areas due to steep slopes with low relief, however, overestimation is still likely in some areas.
- The FOS calculations are strongly influenced by the accuracy and resolution of the input data for material properties, depth to failure, depth to groundwater, and slope angle. Material properties are estimated based on available soils data and a limited amount of published field data, and are worst-case estimates.
- The lidar-based digital elevation model does not distinguish elevation changes due to man-made structures. It would require extensive GIS and field work to locate and remove all these existing structures so many have been retained as a conservative approach.
- Because it is not feasible to collect detailed site-specific information on every landslide, potential mitigating conditions have not been accounted for.
- Debris runout modeling is based on estimates of catchment size and volume. While these are estimates based on our best assessment of the data, differences in these estimates and actual landslide runouts are possible.
- Local conditions may vary substantially from the parameters used to make these maps.
- Interaction of debris flows with buildings can change the direction of flow.
- Large trees in a debris flow can change runout lengths and widths.

ACKNOWLEDGEMENTS

We would like to thank Jacquie Foss from the U.S. Forest Service for her helpful discussions about the data and the time she spent sharing her knowledge of landslides in southeast Alaska. We appreciate Brinnen Carter from the Sitka National Historic Park for his help with logistics and insights about landslides in Sitka. Staff with the City and Borough of Sitka were extremely helpful in tracking down data and providing important input so our results would benefit its citizens. Finally, we wish to acknowledge Cynthia McCoy from FEMA for her guidance during completion of the project and Dennis Staley at the USGS and Bill Burns at DOGAMI for reviews which helped to improve the quality of this product. This project was funded in 2016 by the FEMA Cooperating Technical Partners Program (grant number EMS-2016-CA-00006).

REFERENCES

Becker, M., 2014, Preliminary photo trip report; Starrigavan landslide—September 18/19, 2014: U.S. Forest Service white paper, 20 p. http://kcaw-org.s3.amazonaws.com/wp-content/uploads/2014/09/Starrigavan_landslide_2014.pdf

Bishop, D.M. and Stevens, M.E., 1964, Landslides on logged areas in southeast Alaska: U.S. Department of Agriculture, Northern Forest Experiment Station Research Paper NOR-1, 18 p. https://archive.org/download/CAT31292080/CAT31292080.pdf

Burns W.J., and Madin I.P, 2009, Protocol for inventory mapping of landslide deposits from light detection and ranging (lidar) imagery: Oregon Department of Geology and Mineral Industries Special Paper 42, 30 p. https://www.oregongeology.org/pubs/sp/p-SP-42.htm

Burns W.J., Madin I.P., and Mickelson, K.A., 2012, Protocol for shallow landslide susceptibility mapping: Oregon Department of Geology and Mineral Industries Special Paper 45, 32 p. https://www.oregongeology.org/pubs/sp/p-SP-45.htm

Combellick, R.A., and Long, W.E., 1983, Geologic hazards in southeastern Alaska: an overview: Alaska Division of Geological & Geophysical Surveys Report of Investigation 83-17, 17 p. http://doi.org/10.14509/2356

DGGS Staff, 2013, Elevation Datasets of Alaska: Alaska Division of Geological & Geophysical Surveys Digital Data Series 4, http://maps.dggs.alaska.gov/elevationdata/. http://doi.org/10.14509/25239

Filz, G., 1982, Engineering Properties of Southeast Alaskan Forest soils. Masters of Science in Civil Engineering, Oregon State University, 51p. https://ir.library.oregonstate.edu/downloads/mw22v9355

Geotechdata.info, 2013a, Soil Friction Angle: Geotech.info web page. http://www.geotechdata.info/parameter/angle-of-friction.html (accessed September 14, 2013)

Geotechdata.info, 2013b, Soil Cohesion: Geotech.info web page. http://www.geotechdata.info/parameter/cohesion.html (accessed December 15, 2013).

Golder Associates, 2008, Final report on geotechnical investigation, Whitcomb Heights subdivision, Sitka, Alaska: Report prepared by Golder Associates, Anchorage, Alaska, 073-95050, for USKH, Inc., Juneau, Alaska, 19 p. www.cityofsitka.com/government/departments/parks/documents/StephenFinalGeotechReport.pdf

Gould, A., Wolken, G., Stevens, D., and Whorton, E., 2015, August 18th 2015 Sitka Alaska debris flows: Initial response summary report: Alaska Division of Geological & Geophysical Surveys white paper, 5 p.

Harp, E.L., E.L., Michael, J.A., and Laprade, W.T., 2006, shallow-landslide hazard map of Seattle, Washington: U.S. Geological Survey Open-File Report 2006-1139, 20 p. https://pubs.usgs.gov/of/2006/1139/

Harris, S., 2014, Preliminary field report, Starrigavan Valley landslides: Sitka Conservation Society, 11 p. www.seakecology.org/wp-content/uploads/2014/10/scs_2014_starrigavan_slide_sm.pdf

Iverson, R.M., Schilling, S.P., and Vallance, J.W., 1998, Objective delineation of lahar-inundation hazard zones: GSA Bulletin, v. 110, no. 8, p. 972-984. https://pubs.geoscienceworld.org/gsa/gsabulletin/article-pdf/110/9/972/3383034/i0016-7606-110-8-972.pdf

Johnson, A.C., Swanston, D.N., and McGee, K.E., 2000, Landslide initiation, runout, and deposition within clearcuts and old-growth forests of Alaska: Journal of the American Water Resources Association, v. 36, no. 1, p. 17–30. https://www.fs.fed.us/pnw/pubs/journals/pnw_2000_johnson001.pdf

Schilling, S. P., 1998, LAHARZ: GIS programs for automated mapping of lahar-inundation hazard zones: U.S. Geological Survey Open-File Report 98-638, 80 p. https://pubs.usgs.gov/of/1998/0638/report.pdf

Schroeder W.L., 1983, Geotechnical properties of southeast Alaskan Forest Soils: Oregon State University, Civil Engineering Department, 46 p.

Shannon & Wilson, Inc., 2016, South Kramer Avenue landslide: Jacobs Circle to Emmons

Street, Sitka, Alaska: Shannon & Wilson, Inc., letter report submitted to City and Borough of Sitka, Alaska, 22 p. www.cityofsitka.com/documents/Sitka_SKramerLandslideReport.pdf

United States Department of Agriculture (USDA), 2017, Forest Service Geodata Clearinghouse. https://data.fs.usda.gov/geodata/edw/datasets.php?dsetCategory=geoscientificinformation (Accessed October 2018)

United States Department of Agriculture (USDA), 2018, Natural Resources Conservation Service Web Soil Survey. https://websoilsurvey.nrcs.usda.gov/app/WebSoilSurvey.aspx (Accessed October 2018)

Varnes, D.J., 1978, Slope movement types and processes, in Schuster, R.L., and Krizek, R.J., eds., Landslides analysis and control: Washington, D.C., National Research Council, Transportation Research Board Special Report 176, p. 11–33. http://onlinepubs.trb.org/Onlinepubs/sr/sr176/176.pdf

Yehle, L.A., 1974, Reconnaissance engineering geology of Sitka and vicinity, Alaska, with emphasis on evaluation of earthquake and other geologic hazards: U.S. Geological Survey Open-File Report 74-53, 104 p., 3 sheets, scale 1:9,600. http://dggs.alaska.gov/pubs/id/11000